2018 European Control Conference (ECC)
June 12-15, 2018. Limassol, Cyprus

# Multiscale PLS-based Optimized EW-GLRT for Structural Damage Detection*

Marwa Chaabane[1], Majdi Mansouri[2], Ahmed Ben Hamida[1], Hazem Nounou[3] and Mohamed Nounou[4]

*Abstract*— **In this paper we propose a novel damage detection technique using optimized EWMA (OEWMA)-based GLRT to enhance monitoring of structural systems. The idea behind the developed damage detection algorithm is to incorporate the advantages brought forward by the OEWMA-GLRT damage detection chart with the multiscale representation of the data and input-output model (PLS). The proposed damage detection technique is tested using simulated International Association for Structural Control-American society of Civil engineers (IASC-ASCE) benchmark structure. The results demonstrate the effectiveness of the developed MSPLS-based OEWMA-GLRT when compared to the classical methods.**

## I. INTRODUCTION

For recent years, structural health monitoring (SHM) has been the object of many researchers in civil structures. SHM consists of developing damage detection and characterization strategies based on collected data from installed sensors on the structure. It aims to estimate, identify and / or locate the damage on the structure and to take decisions about the structure' evolution and condition in order to improve its safety. The monitoring phase in SHM goes through two steps, damage detection and diagnosis [1], [2], [3]. In this paper, we will focus on damage detection which has an important role to keep the system safe [4]. In the literature, there is many damage detection methods [5], [6], [7]. These methods can be divided into model based methods [8], [9] and data based methods [10], [11], [12], [13], [14]. Several physical systems of the real civil structure are complex and difficult to construct its model. So the data based methods are very used in damage detection. To do that, modeling and damage detection steps should addressed.

In SHM modeling, the model structure is not available, thus, an empirical data-based modeling techniques will be developed. Latent variable regression (LVR) are the well-known empirical data-based modeling techniques, which include partial least squares (PLS) and principal component analysis (PCA). In this paper, we propose to use an input-output PLS model to take into consideration the information given by the process variables $X$ and the quality variables $Y$. However, most real data include features and noise occurring at different contributions over both time and frequency while the PLS is based on time-domain data. To handle these problems, wavelet-based multiscale representation is used with PLS known as the multiscale PLS (MSPLS) [15]. The MSPLS is a popular statistical method that performs linear form of PLS. Similar to PLS, it is an input output model that reduces process dimension variables. It is based on decomposing data into scales and retaining only significant coefficient of the data at each scale [11]. MSPLS is used to predict quality variables of the system and obtain an accurate input-output model.

Regarding the damage detection problem, several statistical techniques have been developed, such as, generalized likelihood ratio test (GLRT) [16], cumulative sum (CUSUM) chart [17], shewhart control chart [18] and exponentially weighted moving average chart (EWMA) control chart [19], [20], [21].

In our previous works, we have developed PCA, PLS, KPCA, KPLS-based GLRT techniques for fault detection through different applications [13], [22], [23], [24].

The advantage of the EWMA chart in the detection of smaller and moderate damages can be attributed to its extensive process memory. Although, the EWMA chart may be able to better detect smaller damages than the Shewhart chart, it cannot be used to detect a wide range of damage sizes, as it often need to be tuned to detect damages of different sizes. However, EWMA chart usually has some tuning parameters that must be specified by the user such that it is optimal at detecting a specific change size. Therefore, the performance at detecting other change size could be compromised which implies that to effectively apply EWMA chart, the user needs to have relatively good information about the changed parameters (smoothing parameter ($\lambda$) and control width $L$) that would likely happen when the process is out-of-control. Thus, an optimized EWMA (OEWMA) based on the best selection of smoothing parameter ($\lambda$) and control width $L$ will be developed to enhance the monitoring of SHM.

Thus, we propose a new detection chart that combines the advantages of the Optimized EWMA (OEWMA) and GLRT charts. In the proposed OEWMA-GLRT chart, the detection statistic is computed using a more accurate multi-objective function for jointly reducing the missed detection rate (MDR), the false alarm rate (FAR) and the out-of-control average run length ($ARL_1$). Thus, the idea behind an MSPLS-based OEWMA-GLRT damage detection algorithm is to incorporate the advantages brought forward by the proposed OEWMA-GLRT damage detection chart with the

*Qatar National Research Fund (a member of Qatar Foundation)

[1]Advanced Technologies for Medicine and Signals, National Engineering School of Sfax, Tunisia,

[2]Corresponding author, Electrical and Computer Engineering Program, Texas A&M University at Qatar, Doha, Qatar, Tel:+974.4423.0608, Fax: +974.4423.0065, E-mail: majdi.mansouri@qatar.tamu.edu,

[3]Electrical and Computer Engineering Program, Texas A&M University at Qatar, Doha, Qatar,

[4]Chemical Engineering Program, Texas A&M University at Qatar, Doha, Qatar.

multiscale representation of the data and input-output model (PLS).

The damage detection problem was addressed so that the data are first modeled using the MSPLS method and then the damages are detected using OEWMA-GLRT chart. The performance of the developed technique is assessed and compared to the MSPLS-based OEWMA and MSPLS-based GLRT methods using simulated International Association for Structural Control-American society of Civil engineers (IASC-ASCE) benchmark structure. The results demonstrate the effectiveness of the OEWMA-GLRT technique over the MSPLS-based OEWMA and MSPLS-based GLRT methods in terms MDR, FAR and $ARL_1$ values.

The rest of the paper is organized as follows. We first describe the MSPLS method 2. In Section 3, we present the new damage detection chart based on optimized EWMA-GLRT chart. After that, in Section 4, the performance of the proposed damage technique is evaluated using a simulated structural health monitoring benchmarking data. Finally, conclusions are presented in Section 5.

## II. MULTISCALE PARTIAL LEAST SQUARES DESCRIPTION

### A. Partial Least Squares description

Partial least squares is popular statistical method for the modeling and monitoring multivariate data [25]. It aims to construct a statistic model by relating the data matrix $X \in R^{n\times m}$ of the process variable and the data matrix $Y \in R^{n\times p}$ of responses using a linear relationship.
The general underlying model of multivariate PLS is:

$$\begin{aligned} X &= TP^T + E = \sum_{i=1}^{M} t_i p_i^t + E \\ Y &= UQ^T + F = \sum_{j=1}^{M} u_j q_j^t + F \end{aligned} \tag{1}$$

Where, $T$ and $U$ are the orthonormal score matrix of the input $X$ and output $Y$ matrices respectively, $P$ and $Q$ are the loading vectors of the input and output matrices respectively, $E$ and $F$ are the error terms, m is the number of process variables and n is the number of observations in input $(X)$ matrix, $p$ is the number of quality variables in output $(Y)$ matrix and $M$ is the number of retained latent variables.

The key idea of the PLS is projecting high dimensional data onto a low dimensional subspace (defined in terms of latent variables). The latent variables are constructed using the process variables together with the response variables. In order to predict the response, the retained latent variables are used to maximize the covariance between the input and output data(achieve maximum correlation). The PLS model consists of two types of relationships, an outer relations (X and Y individually as 1 and inner relationship, which relates $X$ to $Y$ by $U = BT$. The PLS defines a set of latent variables $t_i$ and $u_i$ $(i = 1, 2, .., M)$ as follows:

$$\begin{aligned} t_i &= X_i w_i \quad (i = 1..M) \\ u_i &= Y_i q_i \end{aligned} \tag{2}$$

where $w_i$ and $q_i$ represent the weight and loading vectors of $X$ and $Y$ respectively. Both $w_i$ and $q_i$ have unit length and are determined by maximizing the covariance between $t_i$and $u_i$. Equation 4 is referred to as the outer relationship for the $X$ and $Y$ blocks respectively. An inner linear relationship is defined as:

$$u_i = b_i t_i \quad (i = 1..M) \tag{3}$$

where $b_i$ is the coefficient of the $i^{th}$ inner regression.

The next step is to deflate $X$ and $Y$ as follows

$$\begin{aligned} X_{i+1} &= X_i - t_i p_i' \quad X_1 = X \\ Y_{i+1} &= Y_i - \hat{b}_i t_i q_i' \quad Y_1 = Y \end{aligned} \tag{4}$$

Letting $\hat{u}_i = \hat{b}_i t_i$ be the prediction of $u_i$, the matrices $X$ and $Y$ can be decomposed as:

$$\begin{aligned} X &= T_M P_M' + E \\ Y &= U_M Q_M' + F \end{aligned} \tag{5}$$

where $P_{m\times M}$ and $Q_{k\times M}$ are the loadings, $T_{n\times M}$ and $U_{n\times M}$ are the scores and the estimated scores for the input and output spaces respectively and $E_{n\times m}$ and $F_{n\times k}$ are the residuals matrices of $X$ and $Y$ respectively.

A number of different algorithms have been proposed for the calculation of the PLS model. The most popular is the NIPALS (Non-linear Iterative Partial Least Squares) algorithm. In this paper, we will use the modified NIPALS algorithm [26]. In this work, we have used the NIPALS algorithm [26] to compute the input-output PLS model.

### B. Multiscale Partial Least Squares

The multiscale process uses the wavelet transformation to decompose the original signal into its multiscale components according to time and frequency characteristics. Comparing to the single scale, the wavelet transformation has the advantage of separating the deterministic and stochastic features from the original signal.
The discrete wavelet transform [27]decomposes the original signal onto two sub-spaces: the approximation sub-space $A$ and the detailed sub-space $D$. These scaled signals are given by projecting the original signal on a set of orthonormal scaling functions of the form,

$$\phi_{ij}(t) = \sqrt{2^{-j}}\phi(2^{-j}t - k) \tag{6}$$

where, $k$ and $j$ are the discretized translation and the dilation parameters,respectively. At the scale $j$, the detailed signal $D_j(t)$ can be determined by passing the original and scaled signals through a high-pass filter (g), and the scaled signals are generated by passing the original and scaled signals through a low-pass filter (h) [27].

Therefore, the original signal can be represented as the sum of all detail signals at all scales and the scaled signal at the coarsest scale as follows:

$$x(t) = \sum_{k=1}^{n2^{-J}} a_{Jk}\phi_{Jk} + \sum_{j=1}^{J}\sum_{k=1}^{n2^{-J}} d_{jk}\psi_{jk}(t) \tag{7}$$

where $j$ is the dilation parameter, $k$ is the translation parameter, $J$ is the maximum number of scales (or decomposition depth) and $n$ is the length of the original signal.
The Multiscale representation has many advantages when applied on autocorrelated or non-Gaussian data [28]. These advantages contain the ability to denoise signals, decorrelate the set of autocorrelated data and make the wavelet coefficients follow a normal distribution. Therefore, the PLS model will be improved using the multiscale representation.

The MSPLS model was firstly developed by [15] with the aim of removing the long term drift in the data set. The MSPLS is implemented by combining the PLS model with the multiscale representation to improve model quality and thus improving the damage detection methods.
Consider the quality variable data matrix $X$, the response variable data matrix $Y$, and the denoised data via multiscale filtering at a scale $(j)$ be $X_j$ and $Y_j$, then the PLS model can be expressed as,

$$Y_j = T_j B_j Q_j^T - F_j \tag{8}$$

where, $X_j \in R^{n*m}$ is the filtered input data matrix at the scale $(j)$, $y_j \in R^{n*1}$ is the filtered output vector at the scale $(j)$ and $F \in R^{m*p}$ is the residuals of output matrices at the scale $(j)$.

The data are decomposed by the discrete wavelet transform, then the PLS model is applied at each scale and the data are reconstructed by selecting only important scale coefficients with statistical threshold.

## III. OPTIMIZED EWMA-GLRT CHART DESCRIPTION

The novel detection chart attempts to combine the advantages of the EWMA and GLRT charts and use a more accurate multi-objective function for jointly reducing the missed detection rate (MDR), the false alarm rate (FAR) and the out-of-control average run length ($ARL_1$) by using the optimal parameters of the EWMA chart.

### A. Classical GLRT detection chart

The damage detection step is done using the residuals evaluated from the MSPLS model. Using the information about the noise distribution of the residuals, the GLRT statistic is computed. To make the decision if a damage is present or not, the test statistic is compared to a computed threshold. Consider the measurement vector $Y \in R^N$:

$$Y = \theta + \epsilon \tag{9}$$

where $\epsilon$ denotes the measurement noise assumed to be Gaussian $\mathcal{N}(0, \sigma^2 I_N)$ and $\theta$ is an unknown parameter.

GLRT is the detector that corresponds to the highest probability of detection ($P_D$) given a fixed false alarm probability for all values of $\theta$. The two-sided hypothesis test could be formulated as:

$$\begin{cases} \mathcal{H}_0 = \{\theta = \theta_0\}, & \text{(null hypothesis)}, \\ \mathcal{H}_1 = \{\theta = \theta_1\}, & \text{(alternative hypothesis)}. \end{cases} \tag{10}$$

The GLRT parameter $\theta$ can be estimated as:

$$\hat{\theta} = \arg\max_\theta (p(Y|\theta)), \tag{11}$$

where, $p$ is the marginal density function of $Y$. The estimated parameters, $\hat{\theta}$, for both hypothesis, are then substituted into the Likelihood Ratio test $G(Y)$ provided in the NP-lemma [29] which yields the GLRT,

$$G(Y) = \frac{p(Y|\hat{\theta}_1)}{p(Y|\hat{\theta}_0)}. \tag{12}$$

The most widely used distribution for random variables is the Gaussian distribution. The residual need to be normalized before the validation or the detection phase. In this case, the normalized residual $R \in R^N$ is assumed to be Gaussian and the vector $Y \in R^N$ is formed by one of $\mathcal{N}(0, \sigma^2 I_N)$ or $\mathcal{N}(\theta \neq 0, \sigma^2 I_N)$ and the hypothesis test (10) can be written as,

$$\begin{cases} \mathcal{H}_0 : R \sim N(0, \sigma^2 I_N) \\ \mathcal{H}_1 : R \sim N(W^T\theta, \sigma^2 I_N), \end{cases} \tag{13}$$

where, $\theta$ is the mean vector, which is the value of the damage and $\sigma^2 > 0$ is the variance, which is assumed to be known.

The GLRT chart yields to the following log-likelihood ratio,

$$\begin{aligned} G(R) &= 2\log \frac{sup_\theta f_{W^T\theta}(R)}{f_{\theta=0}(R)} \\ &= 2\log \left\{ \frac{\sup_\theta \exp\left\{-\frac{1}{2}\|R - W^T\theta\|_2^2\right\}}{\exp\left\{-\|R\|_2^2\right\}} \right\} \\ &= \min_\theta \|R - W^T\theta\|_2^2 + \|R\|_2^2, \end{aligned}$$

which is maximized for $\widehat{\theta}$ to obtain the maximum likelihood estimate of it, which equals $\widehat{\theta} = W^T W^{T^{-1}} R$. Then, the GLRT method replaces the unknown parameter, $\theta$, by its maximum likelihood estimate, which gives the following GLRT statistic,

$$G(R) = \|R - W^T\widehat{\theta}\|_2^2 + \|R\|_2^2 = R^T W^T W^{T^{-1}} R \tag{14}$$

Assuming that the normalized residuals follow a Gaussian distribution, i.e.,

$$R \sim N(W^T\theta, I_N), \tag{15}$$

where $\theta = 0$ under the null hypothesis $\mathcal{H}_0$, then, $G(R) = R^T W^T W^{T^{-1}} R$ will follow a Chi-square distribution i.e.,

$$G(R) = R^T W^T W^{T^{-1}} R \sim \chi_\mu^2(\Lambda), \tag{16}$$

where $\mu = rank(W^T)$ and $\Lambda = (W^T\theta)^T W^T W^{T^{-1}} (W^T\theta)$.

### B. Classical EWMA detection chart

The exponentially weighted moving average chart was firstly introduced by Roberts in 1959 [30]. It is used in process monitoring and diagnosis [31]. The EWMA control chart consists of computing the EWMA statistic and the upper and lower control limits. The EWMA statistic can be computed as follows

$$Z_i = \lambda x_i + (1-\lambda) Z_{i-1} \tag{17}$$

Where $\lambda$ is a smoothing parameter ($0 < \lambda <= 1$) which changes the memory of the detection statistic.

In the same way, the EWMA statistic can be written as a moving average of the current and past observations as follows:

$$Z_i = \lambda \sum_{j=0}^{i-1} (1-\lambda)^j x_{i-j} + (1-\lambda)^i Z_0 \tag{18}$$

This equation shows that the weights assigned to past observations decrease exponentially, giving the name of the EWMA technique.
The upper and lower control limits are defined in terms of the standard deviation of the EWMA statistic and are computed as follows:

$$UCL = \mu_0 + L\sigma_z = \mu_0 + L\sigma \sqrt{\frac{\lambda}{2-\lambda}[1-(1-\lambda)^{2i}]} \tag{19}$$

$$LCL = \mu_0 - L\sigma_z = \mu_0 - L\sigma \sqrt{\frac{\lambda}{2-\lambda}[1-(1-\lambda)^{2i}]} \tag{20}$$

When the EWMA statistic goes beyond the range of the control limits, the process is considered to be out of control. To use the EWMA method, the choice of the smoothing parameter needs to be made carefully. However, in practice, the optimum choice of the smoothing parameter depends on the size of the mean shift to be detected. For large mean shifts, large values of $\lambda$ are needed, while smaller values of $\lambda$ are needed to detect smaller mean shifts more quickly.

### C. Multiobjective-based Optimized EWMA-GLRT detection chart

The optimized EWMA statistic consists of computing the optimized smoothing parameters of EWMA $\hat{\lambda}$ and $\hat{L}$.
For this purpose, a multi-objective optimization is used to compute the optimal values $\hat{\lambda}$ and $\hat{L}$. The aim is to jointly optimize the smoothing parameter $\lambda$ and control width $L$ based on multi-objective optimization (MOO). The MOO is addressed using three objective functions:

- Missed Detection Rate (MDR) (%): percentage of damaged observations undetected,
- False Alarm Rate (FAR) (%): percentage of wrong damage declared in damage free region, and
- Average Run Length ($ARL_1$): average number of observation plotted on the control chart before a damage is indicated (e.g. a point plotted outside the control limit).

Let denote ($D_E = [\lambda, L]$) the decision variables or optimization vector.
To select the optimal smoothing parameters of EWMA $\hat{\lambda}$ and $\hat{L}$, we build a MOO scheme containing three objective functions (DAR, FAR and $ARL_1$). This scheme gives a trade-off between the three metrics. The solutions of the MOO are called Pareto-optimal or non-dominated solutions. Theses solutions are all important and constitute global optimum solutions.The non-dominated optimization problem consists of finding the optimal solutions via a minimization problem. The MOO finds the vector $\hat{D}_E$ of decision variables that simultaneously minimizes the three objective functions MDR, FAR and $ARL_1$. A non-dominated solution $D_{i,E}$ is said to dominate $D_{j,E}$ if $\forall k \in 1, 2, ..f_k(D_{i,E}) \leq f_k(D_{j,E})$ and $\exists k \in 1, 2, ..$ such that $f_k(D_{i,E}) \leq f_k(D_{j,E})$, where, $f_k$ denotes the $k$-th objective function. The non-dominated ones $D_{ND}$ from all the solutions $D_E$ are not dominated by any member of the set $D_E$. Hence, this method enables to select the optimal vector $\hat{D}_E$ which minimizes MDR, FAR and $ARL_1$ as follows:

$$\hat{D}_E = \underset{D_E \in R^N}{\arg\min} \left[FAR(D_E), MDR(D_E), ARL_1(D_E)\right]. \tag{21}$$

After selecting these smoothing parameters, we calculate the OEWMA statistic.

The optimized EWMA-GLRT statistic ($OEG$) can be computed as:

$$OEG(R) = \alpha \frac{GLR(R)}{G_\alpha} + (1-\alpha)\frac{OEWMA(R)}{UCL} \tag{22}$$

where $\alpha$ is a weight parameter ($0 < \alpha < 1$), $G_\alpha$ and UCL are the upper limits of GLR and OEWMA statistic charts. The optimal value of $\alpha$ that provides the best detection performance is selected.

To define the threshold of the new chart, it is necessary to compute the distribution of the test statistic ($OEG$) [32].

If the OEWMA-GLRT statistic $OEG$ value is less than the computed threshold value $OEG_\alpha$ under null hypothesis, there is no damage and if $OEG$ statistic is higher than threshold value, alternative hypothesis is correct and damage is declared in the process.

The algorithm that presents the proposed OEWMA-GLRT is shown in Algorithm 1.

## IV. PROPOSED MSPLS BASED OEWMA-GLRT TECHNIQUE WITH APPLICATION TO SHM SYSTEM

The MSPLS based OEWMA-GLRT consists of incorporating the advantages from the MSPLS model with the OEWMA-GLRT damage detection chart. In the proposed method, the MSPLS model is constructed. Then in order to perform the damage detection accuracies, the OEWMA-GLRT is applied with using the optimal non-dominated solutions. This MSPLS-based OEWMA-GLRT damage detection technique aims to simultaneously detect damage with minimum MDR, FAR and $ARL_1$

**Algorithm 1:** OEWMA-GLRT algorithm

1) set $L = 0.1, 0.2, 0.3, .., 3$ and $\lambda = 0.05, 0.1, 0.15, .., 1$
2) Compute the EWMA charts for all $L$ and $\lambda$
3) Compute MDR, FAR and $ARL_1$ for all $L$ and $\lambda$
4) Generate and plot a Pareto front
5) Extract the non-dominated solutions
6) Compute the corresponding $\hat{L}$ and $\hat{\lambda}$ that correspond to MDR=FAR=$ARL_1$
7) Compute the OEWMA statistic using $\hat{L}$ and $\hat{\lambda}$
8) Compute the new chart OEWMA-GLRT $OEG = \alpha \frac{GLR(R)}{G_\alpha} + (1-\alpha)\frac{OEWMA(R)}{UCL}$
9) Compute MDR, FAR and $ARL_1$ for all $\alpha$ varying from [0..1]
10) Choose the best $\hat{\alpha}$ that minimizes MDR, FAR and $ARL_1$
11) Re-compute the chart OEWMA-GLRT $OEG = \hat{\alpha} \frac{GLR(R)}{G_\alpha} + (1-\hat{\alpha})\frac{OEWMA(R)}{UCL}$
12) Compute the OEWMA-GLRT threshold.

The effectiveness of the MSPLS for damage detection purposes will be demonstrated through a simulated benchmark IASC-ASCE model.

The simulated benchmark process consists of four-story, two-bay by two bay structure provided by the IASC-ASCE [33]. A diagram of the analytical model is shown in Figure 1.

The benchmark gives an analytical models based on the

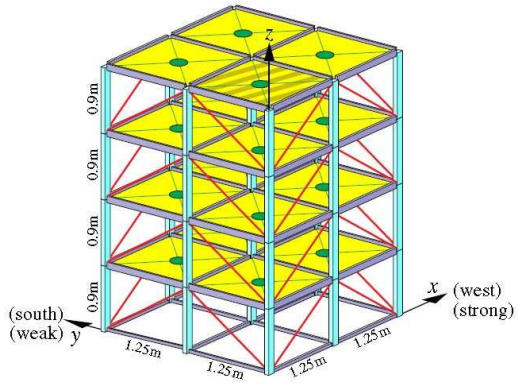


Fig. 1. Steel-frame scale structure

structure 12 DOF shear-building model. In this model, the floors (floor beams and floor slabs) move as rigid bodies, with translation in the $x$ - and $y$ -directions and rotation $\theta$ about the center column. Thus, there are three degrees-of-freedom per floor. The columns are modeled as linear elastic Euler-Bernoulli beams, and the braces as axial bars.
The data generated by the model contains:

1) The inputs: 4 forces: the loading in the $y$-direction at the each floor.
2) The outputs: 16 accelerations: 2 each in the $x$ and $y$ direction per floor.

As a data set, we use the case of 12 DOF (symmetric) which loads at all stories with damping ration equals to 0.01, noise level equals to 10, force intensity equals to $150Hz$ and time step size equals to $0.001s$. We also use 1024 samples for training and 1024 samples for testing [33]. The training input generated data are shown in Figure 2.

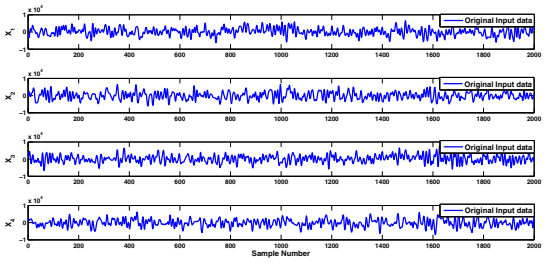


Fig. 2. Training input generated data

For the testing output data, we add an additive damage of $5\sigma$ magnitude in the third variable $X_3$ to test damage detection accuracies.

The best decomposition depth is equal to 3 in order to get good detection abilities with lower MDR, FAR and $ARL_1$.

In this case, a damage of magnitude $3\sigma$ is introduced in $X_3$ between samples 800-1000. Figures 3 to 6 show the detection comparison between PLS-based GLRT, PLS-based OEWMA, PLS-based OEWMA-GLRT and MSPLS-based OEWMA-GLRT methods. We can show from these results that the both the OEWMA and OEWMA-GLRT charts provide better detection results when compared to the conventional GLRT chart. The detection performance based multiscale representation shows good improvement compared to the classical one. This is due to that the use of multiscale representation may reduce the false alarm and missed detection rates.

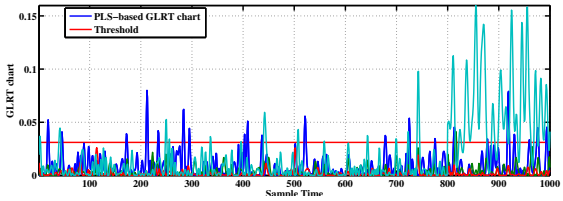


Fig. 3. Time evolution of detection using PLS-based GLRT method

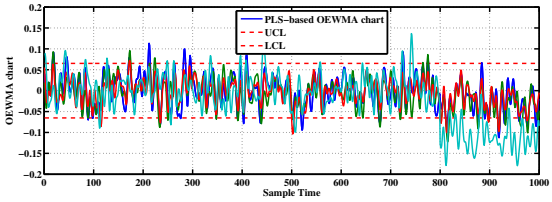


Fig. 4. Time evolution of detection using PLS-based OEWMA method

## V. CONCLUSIONS

In this paper, we proposed a new structural damage detection technique called multiscale Partial Least Squares (MSPLS)-based on optimized exponentially weighted moving average (OEWMA)-generalized likelihood ratio test (GLRT). The damage detection problem was addressed so

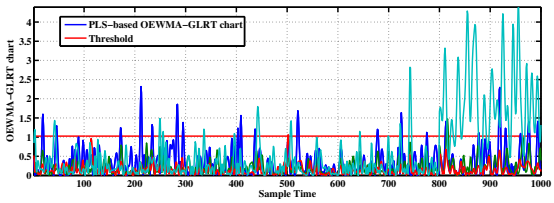


Fig. 5. Time evolution of detection using PLS-based OEWMA-GLRT method

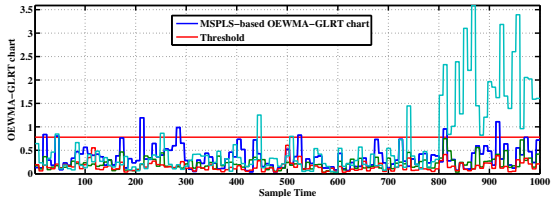


Fig. 6. Time evolution of detection using MSPLS-based OEWMA-GLRT method

that the data are first modeled using the MSPLS method and then the damages are detected using the OEWMA-GLRT chart. The performance of the developed technique is assessed using simulated International Association for Structural Control-American society of Civil engineers (IASC-ASCE) benchmark structure.

## ACKNOWLEDGMENT

This work was supported by Qatar National Research Fund (a member of Qatar Foundation) under the NPRP grant NPRP9 − 330 − 2 − 140.

## REFERENCES

[1] Y. Lei, A. S. Kiremidjian, K. K. Nair, J. P. Lynch, K. H. Law, E. Carryer, and A. Kottapalli, "Statistical damage detection using time series analysis on a structural health monitoring benchmark problem," 2003.

[2] J.-C. Malela-Majika and E. Rapoo, "Distribution-free mixed cumulative sum-exponentially weighted moving average control charts for detecting mean shifts," *Quality and Reliability Engineering International*.

[3] S.-F. Yang and S.-H. Wu, "A double sampling scheme for process variability monitoring," *Quality and Reliability Engineering International*.

[4] B. Zaman, M. Riaz, N. Abbas, and R. J. Does, "Mixed cumulative sum–exponentially weighted moving average control charts: an efficient way of monitoring process location," *Quality and Reliability Engineering International*, vol. 31, no. 8, pp. 1407–1421, 2015.

[5] R. V. León and W. David Clark, "Detecting changes in field reliability using data from a complex factory screen," *Quality Engineering*, vol. 17, no. 1, pp. 67–75, 2004.

[6] Z. Dzunic, J. G. Chen, H. Mobahi, O. Büyüköztürk, and J. W. Fisher, "A bayesian state-space approach for damage detection and classification," *Mechanical Systems and Signal Processing*, vol. 96, pp. 239–259, 2017.

[7] X. Li, L. Wang, S. Law, and Z. Nie, "Covariance of dynamic strain responses for structural damage detection," *Mechanical Systems and Signal Processing*, vol. 95, pp. 90–105, 2017.

[8] J. Li, J. Deng, and W. Xie, "Damage detection with streamlined structural health monitoring data," *Sensors*, vol. 15, no. 4, pp. 8832–8851, 2015.

[9] A.-M. Yan, P. De Boe, and J.-C. Golinval, "Structural damage diagnosis by kalman model based on stochastic subspace identification," *Structural Health Monitoring*, vol. 3, no. 2, pp. 103–119, 2004.

[10] M. Mansouri, M. N. Nounou, and H. N. Nounou, "Improved statistical fault detection technique and application to biological phenomena modeled by s-systems," *IEEE transactions on nanobioscience*, vol. 16, no. 6, pp. 504–512, 2017.

[11] ——, "Multiscale kernel pls-based exponentially weighted-glrt and its application to fault detection," *IEEE Transactions on Emerging Topics in Computational Intelligence*, 2017.

[12] R. Fezai, M. Mansouri, O. Taouali, M. F. Harkat, and N. Bouguila, "Online reduced kernel principal component analysis for process monitoring," *Journal of Process Control*, vol. 61, pp. 1–11, 2018.

[13] M.-F. Harkat, M. Mansouri, M. Nounou, and H. Nounou, "Enhanced data validation strategy of air quality monitoring network," *Environmental research*, vol. 160, pp. 183–194, 2018.

[14] M. Mansouri, M.-F. Harkat, M. Nounou, and H. Nounou, "Midpoint-radii principal component analysis-based ewma and application to air quality monitoring network," *Chemometrics and Intelligent Laboratory Systems*, 2018.

[15] P. Teppola and P. Minkkinen, "Wavelet-pls regression models for both exploratory data analysis and process monitoring," *Journal of Chemometrics*, vol. 14, no. 5-6, pp. 383–399, 2000.

[16] F. Gustafsson, "The marginalized likelihood ratio test for detecting abrupt changes," *IEEE Transactions on Automatic Control*, vol. 41, no. 1, pp. 66–78, 1996.

[17] E. S. Page, "Continuous inspection schemes," *Biometrika*, pp. 100–115, 1954.

[18] M. Hart and R. Hart, "Shewhart control charts for individuals with time-ordered data," in *Frontiers in Statistical Quality Control 4*. Springer, 1992, pp. 123–137.

[19] S. W. Roberts, "Control chart tests based on geometric moving averages," *Technometrics*, vol. 1, no. 3, pp. 239–250, 1959.

[20] S. V. Crowder and M. D. Hamilton, "An ewma for monitoring a process standard deviation," *Journal of Quality Technology*, vol. 24, no. 1, pp. 12–21, 1992.

[21] J. S. Hunter, "The exponentially weighted moving average." *Journal of Quality Technology*, vol. 18, no. 4, pp. 203–210, 1986.

[22] M. Mansouri, M. Nounou, H. Nounou, and K. Nazmul, "Kernel pca-based glrt for nonlinear fault detection of chemical processes," *Journal of Loss Prevention in the Process Industries*, vol. 26, no. 1, pp. 129–139, 2016.

[23] M. Mansouri, H. Nounou, M. F. Harkat, and M. Nounou, "Fault detection of chemical processes using improved generalized likelihood ratio test," in *Digital Signal Processing (DSP), 2017 22nd International Conference on*. IEEE, 2017, pp. 1–5.

[24] C. Botre, M. Mansouri, M. N. Karim, H. Nounou, and M. Nounou, "Multiscale pls-based glrt for fault detection of chemical processes," *Journal of Loss Prevention in the Process Industries*, vol. 46, pp. 143–153, 2017.

[25] S. Wold, M. Sjstrm, and L. Eriksson, "Pls-regression: a basic tool of chemometrics," *Chemometrics and Intelligent Laboratory Systems*, vol. 58, no. 2, pp. 109 – 130, 2001.

[26] T. Kourti and J. F. MacGregor, "Process analysis, monitoring and diagnosis, using multivariate projection methods," *Chemometrics and Intelligent Laboratory Systems*, vol. 28, no. 1, pp. 3 – 21, 1995.

[27] G. Nason, "Wavelet shrinkage: asymptopia?" *Journal of the Royal Statistical Society: Series B (Statistical Methodology)*, vol. 57, pp. 341 – 342, 1995.

[28] R. GANESAN, T. K. DAS, and V. VENKATARAMAN, "Wavelet-based multiscale statistical process monitoring: A literature review," *IIE Transactions*, vol. 36, no. 9, pp. 787–806, 2004.

[29] S. M. Kay, "Fundamentals of statistical signal processing: Detection theory, vol. 2," 1998.

[30] S. W. Roberts, "Control chart tests based on geometric moving averages," *Technometrics*, vol. 1, no. 3, pp. 239–250, 1959.

[31] P. E. Maravelakis and P. Castagliola, "An ewma chart for monitoring the process standard deviation when parameters are estimated," *Comput. Stat. Data Anal.*, vol. 53, no. 7, pp. 2653–2664, May 2009.

[32] G. Rahman, S. Mubeen, and A. Rehman, "Generalization of chi-square distribution," *Journal of Statistics Applications & Probability*, vol. 4, no. 1, p. 119, 2015.

[33] E. A. Johnson, H.-F. Lam, L. S. Katafygiotis, and J. L. Beck, "Phase i iasc-asce structural health monitoring benchmark problem using simulated data," *Journal of engineering mechanics*, vol. 130, no. 1, pp. 3–15, 2004.